

1 **Observed emergence of the climate change signal: from the familiar to the unknown**
2 **E. Hawkins¹, D. Frame², L. Harrington^{2,3}, M. Joshi⁴, A. King⁵, M. Rojas⁶, and R. Sutton¹**

3 ¹ National Centre for Atmospheric Science, Dept. of Meteorology, University of Reading, UK.

4 ² New Zealand Climate Change Research Institute, Victoria University of Wellington, New
5 Zealand.

6 ³ Environmental Change Institute, University of Oxford, South Parks Road, Oxford, UK.

7 ⁴ Climatic Research Unit, School of Environmental Sciences, University of East Anglia, UK.

8 ⁵ School of Earth Sciences and ARC Centre of Excellence for Climate Extremes, University of
9 Melbourne, Australia.

10 ⁶ Department of Geophysics and Centre for Climate and Resilience Research, CR2, University of
11 Chile, Chile.

12 Corresponding author: Ed Hawkins (e.hawkins@reading.ac.uk)

13 **Key Points:**

- 14 • The signal of changes in observed temperature and rainfall due to global warming has
15 clearly emerged in many regions and at meso-scales
- 16 • Tropical regions have experienced the largest changes in temperature relative to the
17 amplitude of internal variability
- 18 • Signals of increasing extreme rainfall are emerging more quickly than signals in mean
19 rainfall over many parts of the UK

20

21

22 Abstract

23 Changes in climate are usually considered in terms of trends or differences over time. However,
24 for many impacts requiring adaptation, it is the amplitude of the change relative to the local
25 amplitude of climate variability which is more relevant. Here, we develop the concept of ‘signal-
26 to-noise’ in observations of local temperature, highlighting that many regions are already
27 experiencing a climate which would be ‘unknown’ by late 19th century standards. The emergence
28 of observed temperature changes over both land and ocean is clearest in tropical regions, in
29 contrast to the regions of largest change which are in the northern extra-tropics – broadly
30 consistent with climate model simulations. Significant increases and decreases in rainfall have
31 also already emerged in different regions with the UK experiencing a shift towards more extreme
32 rainfall events, a signal which is emerging more clearly in some places than the changes in mean
33 rainfall.

34 Plain Language Summary

35 Changes in climate are translated into impacts on society not just through the amount of change,
36 but how this change compares to the variations in climate that society is used to. Here we
37 demonstrate that significant changes, when compared to the size of past variations, are present in
38 both temperature and rainfall observations over many parts of the world.

39 1 Introduction

40 It was first noted that surface air temperatures were increasing at both local and global scales
41 more than 80 years ago [*Kincer* 1933, *Callendar* 1938]. At the time it was unclear whether the
42 observed changes were part of a longer term trend or a natural fluctuation – the ‘signal’ had not
43 yet clearly emerged from the ‘noise’ of variability – although *Callendar* [1938] did suggest that
44 the increase in atmospheric carbon dioxide concentrations was partly to blame.

45 The concept of the emergence of a climate change signal has since been discussed extensively,
46 often linked with the detection & attribution of climatic changes. For example, *Madden &*
47 *Ramanathan* [1980] and *Wigley & Jones* [1981] could not robustly detect the carbon dioxide
48 warming signal, but *Hansen et al.* [1988] predicted that the ratio of temperature change and the
49 magnitude of interannual variability – the signal-to-noise ratio – would be above 3 in large parts
50 of the tropics by the 2010s, with smaller values over high latitude land regions. *Mahlstein et al.*
51 [2011, 2012] subsequently demonstrated that the signal had indeed emerged in the observations,
52 especially in the tropics in boreal summer, and with a similar pattern to that expected from
53 climate model simulations. *Lehner et al.* [2017] subsequently highlighted emergence of observed
54 temperature changes in both winter and summer in the northern extra-tropics. Significant
55 changes in precipitation are often harder to detect because both thermodynamic and dynamic
56 factors are crucial [e.g. *Zappa & Shepherd*, 2017] and because internal variability in precipitation
57 is larger. However, precipitation changes are apparent in some regions [e.g. *Zhang et al.* 2007]
58 including in extremes [e.g. *Min et al.* 2011].

59 Many studies have also considered when further changes in climate will emerge, for both mean
60 temperature [*Mahlstein et al.* 2011, *Hawkins & Sutton* 2012] and precipitation [*Giorgi & Bi*
61 2009, *Fischer et al.* 2014]. Other studies have considered when changes in climate extremes
62 should have emerged in the past [*King et al.* 2015] or future [*Diffenbaugh & Scherer* 2011,

63 *Fischer et al.* 2014]. However, rather than examine the timing of any climate emergence, we
 64 focus here on the related quantity – signal-to-noise.

65 The clearest emergence of warming – and largest signal-to-noise values – tend to be found in the
 66 tropics, which are regions with large and vulnerable populations [*Frame et al.* 2017, *Harrington*
 67 *et al.* 2017]. Signal-to-noise (S/N) is important for climate impacts, especially for ecosystems
 68 which have a limited ability to adapt and so large changes outside past experience could be
 69 particularly harmful [*Deutsch et al.* 2008; *Beaumont et al.* 2011]. Crop growing areas also face
 70 unprecedented heat [*Battisti & Naylor* 2009] and changes in rainfall which may move outside
 71 past experiences [*Rojas et al.* 2019]. The impacts of shifts in snowfall [*Diffenbaugh et al.* 2012]
 72 and Köppen–Geiger zones [*Mahlstein et al.* 2013] have also been discussed in terms related to
 73 the natural variability of the local conditions. Quantifying the changes that have already occurred
 74 may help determine which regions are suffering the largest adverse consequences of a warming
 75 world.

76 Here, we revisit the question of where and how the climate change signal is emerging from the
 77 background noise of internal variability. In contrast to most previous studies we focus our
 78 analysis on observational datasets of temperature and precipitation, with model simulations used
 79 only to test the methodology.

80 **2. Observed emergence and signal-to-noise**

81 **2.1 Methodology**

82 Our aim is to produce estimates of signal-to-noise (S/N) for changes in observed climate
 83 variables without utilising data from any climate model simulations. The simple approach
 84 adopted is to linearly regress local variations in climate onto annual global mean surface
 85 temperature change (GMST), i.e.

$$86 \quad L(t) = \alpha G(t) + \beta,$$

87 where $L(t)$ is the local change (in temperature or precipitation) over time, $G(t)$ is a smoothed
 88 version of GMST change over the same period, α defines the linear scaling between L and G ,
 89 and β is a constant. *Sutton et al.* [2015] highlighted that a large fraction of variance in local
 90 climate changes can be represented by GMST changes, and *Fischer et al.* [2014] demonstrated
 91 that a similar regression approach provided robust estimates of S/N when examining future
 92 changes in precipitation in climate model simulations.

93 For $G(t)$ we use GMST from the Berkeley Earth temperature dataset for 1850-2018 (*Rohde et al.*
 94 [2013], combined with HadSST3 from *Kennedy et al.* [2011]), relative to the mean of 1850-
 95 1900, and smoothed with a lowess filter of 41-years to highlight the long-term variations (Figure
 96 1a). The conclusions are insensitive to whether the smoothing parameter is slightly larger or
 97 smaller. The ‘signal’ of global temperature change is defined as the value of the smoothed

98 GMST in 2018 ($G_{2018} = 1.19\text{K}$), the ‘signal’ of local climate change described by GMST is αG
 99 and the ‘noise’ is defined as the standard deviation of the residuals ($L - \alpha G$).

100 Although we do not formally attribute the observed change in GMST, and hence local changes,
 101 to particular radiative forcings or feedbacks, applying the method of *Haustein et al.* [2017] to
 102 derive a GMST change that is attributable to human activity gives 1.22K, similar to G_{2018} .
 103 Although 1850-1900 is often considered as a proxy for ‘pre-industrial’ GMST, the *Haustein et al.*
 104 *et al.* [2017] approach also suggests an additional anthropogenic warming of around 0.05K
 105 occurred between 1750 and 1850-1900, based on radiative forcing estimates back to 1750.
 106 Although this plausible pre-1850 attributable warming is not included in our analysis, we refer to
 107 the 1850-1900 period as the early-industrial era, rather than pre-industrial.

108 **2.2 Example for annual mean temperatures in Oxford**

109 To demonstrate our approach we consider a case study of temperature change in Oxford, UK.
 110 *Burt & Burt* [2019] produced an extended temperature record for the Oxford Radcliffe
 111 Observatory with annual means available for 1814-2018. The temporal evolution of GMST and
 112 temperatures in Oxford are similar, showing that the ‘fingerprint’ of GMST change is clearly
 113 visible at the spatial scale of a single continuous weather station, although with more noise at the
 114 local scale (Figure 1b, also see *Sutton et al.* [2015]). We note that there is likely an urban heat
 115 island influence on temperatures in Oxford of around 0.1-0.2K [*Burt & Burt* 2019].

116 We regress this local temperature dataset onto smoothed GMST and obtain $\alpha = 1.45 \pm 0.25$ (95%
 117 confidence interval). The ‘signal’ for Oxford is $\alpha G_{2018} = 1.72 \pm 0.30\text{K}$ and the ‘noise’, i.e. the
 118 local variations that are not explained by GMST variations, is 0.54K. Oxford therefore exhibits a
 119 S/N ratio of 3.2 ± 0.5 (Figure 1b).

120 We adopt the language of *Frame et al.* [2017] to describe how the climate has changed from
 121 being familiar, to being ‘unusual’ relative to lived experience ($S/N > 2$), ‘unknown’ ($S/N > 3$),
 122 and here we introduce ‘inconceivable’ for S/N values above 5 (Fig. S1). Using this terminology,
 123 temperatures in Oxford have become unknown relative to the early-industrial era. Two other
 124 regional examples are illustrated in Fig. S2.

125 **2.3 Local climate data and methodological tests**

126 We perform a similar S/N analysis for each land and ocean gridpoint in the Berkeley Earth
 127 temperature dataset (1850-2018) and in the GPCCv2018 land precipitation dataset (1891-2016,
 128 *Schneider et al.* [2017]). We use the $1^\circ \times 1^\circ$ datasets for both Berkeley Earth and GPCC. We also
 129 use the HadUK-Grid dataset for the UK [*Hollis et al.* 2019] at 25km spatial resolution for
 130 monthly (1862-2017) and daily (1891-2017) precipitation data to examine changes in mean
 131 rainfall and extremes. Note that smoothed GMST (1850-2018) is used as G for both local
 132 temperature and precipitation analyses.

133 As the local data is not necessarily available for all years back to 1850 we perform the regression
 134 only over the period where local temperatures or precipitation are defined. The signal relative to
 135 the early-industrial era can still be calculated assuming that the estimated regression parameter
 136 (α), is representative for the whole period, i.e. the signal is always αG_{2018} , irrespective of the

137 time period used to calculate α . However, we require that there must be at least 100 years of
138 local climate data available.

139 We test our methodology using a large ensemble of climate simulations for the historical period
140 [Maier et al. 2019], specifically to examine the uncertainty due to internal variability in derived
141 S/N values for temperature and precipitation. Figs. S3 and S4 demonstrate that the methodology
142 produces S/N values with small uncertainties (typically <0.4 over land regions) and robust
143 patterns.

144 **3. Emergence of unknown temperatures**

145 The map of the current observed signal of annual temperature change, relative to the early-
146 industrial era, is shown in Figure 2a. It shows the familiar pattern of more warming over land
147 than over the oceans, more warming at high northern latitudes, and less warming in the tropical
148 regions and the southern hemisphere. Virtually all locations have experienced more than 1K
149 change since the early-industrial era, and many regions have exceeded 2K. The estimated noise
150 shows a similar pattern with larger variability at higher northern latitudes, but the differences
151 between the tropics and extra-tropics are more pronounced than for the signal (Figure 2b).

152 The ratio of these two patterns results in a signal-to-noise (S/N) map with the largest values in
153 the tropical regions (Figure 2c). Although these areas generally have smaller signals than higher
154 latitude regions, they have experienced a larger amplitude change relative to the (smaller)
155 background variations in temperature than other regions. This is important as societies,
156 infrastructure and ecosystems are often adapted for the range of local climate experienced. S/N
157 measures how far the climate is being shifted from that past range; the climate in large parts of
158 the tropics has shifted such that the mean climate would have been inconceivable in the early-
159 industrial era. More than half of the land area has experienced S/N above 3, and so has moved
160 into a climate that is unknown by early-industrial standards (Fig. S5).

161 Over the oceans the largest S/N values are found in the tropical Atlantic and tropical Indian
162 Oceans. Fish species such as tuna have already been seen to be moving away from the tropics to
163 the sub-tropics, likely to avoid these warmer waters [Monllor-Hurtado et al. 2017]. Large parts
164 of the North Atlantic have seen little warming overall, likely due to changes in ocean circulation
165 providing a local cooling influence to offset global warming [e.g. Dima & Lohmann 2010].

166 Although there are variations in magnitude, the estimated S/N pattern is relatively robust to the
167 choice of temperature dataset [Morice et al. 2012, Cowtan & Way 2014, Lenssen et al. 2019,
168 Zhang et al. 2019]. However, there are notable local differences between datasets over south-east
169 USA and parts of South America (Fig. S6). The overall observed emergence pattern is broadly
170 similar to that found in models under future climate change scenarios [Frame et al., 2017]
171 though there are regional-scale differences; especially in the oceans but over some land areas
172 too.

173 When considering how changes in climate may be experienced, it may in many cases be more
174 relevant to examine seasonal or monthly timescales, depending on the impact being considered.
175 For example, Figure 3 shows that S/N values can still be significant for monthly average
176 temperatures. Again, the largest S/N values are found in the tropics and tend to be larger for the

177 climatologically warmest month than the climatologically coldest month for each location. This
178 is because weather variability tends to be larger in the colder months. Around 40% of land areas
179 have moved into an unusual climate in their warmest months, and 20% in the coldest months
180 (Fig. S5). This suggests a comparatively large increase in likelihood of heat-related extreme
181 events in already warm months of already hot countries. One example is south-east Asia where
182 the S/N values are large and the combined effects of El Nino events and climate change on
183 extreme heat in the warmest months of the year has previously been noted [*Thirumalai et al.*
184 2017].

185 **4. Emergence of unusual precipitation amounts**

186 The S/N analysis is repeated for annual mean precipitation using the GPCP dataset. In this case,
187 some regions are getting significantly wetter and others are getting significantly drier (Figure 4)
188 but, unsurprisingly, the signals are less clear than for temperature. Notable emergence of
189 ‘unfamiliar’ (S/N > 1) or unusual precipitation changes are observed in west Africa, Brazil, Chile
190 and south-west Australia (drier), and the northern high latitudes and Argentina (wetter). The
191 seasonal values of S/N are shown in Fig. S7. The changes in several of these regions have been
192 discussed as being consistent with the expected response to increased greenhouse gas forcing,
193 e.g. for south-west Australia [*Delworth & Zeng 2014*], for Chile [*Boisier et al. 2016*] and the
194 northern extra-tropics [*Zhang et al. 2007*].

195 To demonstrate that this framework can be applied to a range of gridded datasets and spatial
196 scales, we consider one small region in more detail. The UK has a gridded rainfall dataset
197 available, covering 1891-2017 (daily) and 1862-2017 (monthly), which is suitable for examining
198 changes in mean and extreme rainfall [*Hollis et al. 2019*].

199 Figure 5 shows the signal and S/N for annual mean rainfall, highlighting a tendency for
200 increasing rainfall in large parts of the northern UK and the western coasts of up to 20% per K of
201 GMST change. The corresponding S/N values exceed 1 in several areas, and these tend to be
202 mountainous regions. Fig. S8 shows the seasonal mean S/N values.

203 When considering the wettest day of the year (RX1day) as $L(t)$, there is a clear signal of
204 increasing extreme rainfall, but the pattern is strikingly different to the mean. This signal is
205 visible across large parts of the UK, even in regions where there are only small changes in mean
206 rainfall. The signal has only clearly emerged in a few locations (Fig. 5) but the spatial average of
207 RX1day across the UK suggests an increase in extreme rainfall amounts of around 4mm (or
208 11%) per K of GMST change (Fig. S9), which is around 8% per K of UK temperature change,
209 approximately consistent with Clausius-Clapeyron expectations [*Pall et al. 2007*].

210 These findings are consistent with *Min et al.* [2011] who showed that the signal of changes in
211 extreme rainfall were detectable and attributable to human activity over large parts of the
212 northern hemisphere land areas, and with *Fischer et al.* [2014] used climate model simulations to
213 suggest that emergence of changes in extreme rainfall can occur earlier than changes in mean
214 rainfall. Continued recovery of millions of undigitized weather observations, including for daily

215 rainfall, will improve and lengthen these gridded datasets [e.g. *Ashcroft et al.* 2018; *Hawkins et*
216 *al.* 2019].

217 **5. Summary and discussion**

218 We have estimated the signal-to-noise ratio (S/N) of observed temperature and precipitation
219 changes since the early-industrial era (1850-1900). Although we do not formally attribute these
220 local changes to specific radiative forcings or feedbacks, the emergence of significantly different
221 climates is related to increases in GMST, which itself is largely due to anthropogenic factors
222 [e.g. *IPCC* 2018].

223 Consistent with previous studies and expectations from climate model simulations, the largest
224 S/N values for historical temperature changes are seen in the tropical regions, over both land and
225 ocean. Large regions have already experienced a shift to a climate state that is unknown, and
226 even inconceivable, compared to that in the late 19th century. These signals of change are also
227 clear in monthly average temperatures, with warmer months showing more significant changes.

228 Precipitation signals are emerging in several regions when considering observed rainfall changes,
229 particularly West Africa, parts of South America and northern Eurasia. Some regions in South
230 America and central Africa exhibit simultaneously high S/N for temperature ($S/N > 4$) and
231 significantly drier precipitation ($S/N < -1$) which may compound impacts.

232 As a demonstration of the methods in a data-rich region, and over a range of spatial scales, our
233 analysis shows there are clear shifts towards more annual rainfall over the UK, focussed over
234 northern and western areas. Significant increases in extreme heavy rainfall are emerging over
235 large parts of the UK and are emerging more quickly than changes in mean rainfall in some
236 places. The magnitude of the increase in extreme rainfall (~8% per K of local temperature
237 change) is approximately consistent with expectations from the Clausius-Clapeyron relationship.

238 Many of the largest global shifts in climate, relative to the background variability, are found in
239 countries with large, vulnerable populations, and this will be exacerbated if policy targets such as
240 those in the Paris Agreement are not met [*Frame et al.* 2017, *King & Harrington* 2018]. There
241 are also implications for ecosystems in these regions, which may not be able to adapt to such an
242 unknown climate, especially given the rates of change. The rates of change of signal-to-noise to
243 which societies and ecosystems can adapt is an important topic for future analyses.

244 **Acknowledgments**

245 We thank Nicola Maher for providing the MPI large ensemble data. EH and RS were supported
246 by the National Centre for Atmospheric Science, and EH was funded by the INDECIS project.
247 ADK was funded by the Australian Research Council (DE180100638). MJ is funded by UK
248 Natural Environment Research Council grants NE/S004645/1 and NE/N018486/1. MR
249 acknowledges funding from FONDAP-CONICYT 15110009. DJF and LJH were supported by
250 the Whakahura project funded by the Endeavour Fund (contract RTVU1906). The datasets used
251 in this paper are freely available online: Berkeley Earth (<http://berkeleyearth.org>), Cowtan &
252 Way (<https://www-users.york.ac.uk/~kdc3/papers/coverage2013/series.html>), HadCRUT4
253 (<https://www.metoffice.gov.uk/hadobs/hadcrut4/>), GISTEMP
254 (<https://data.giss.nasa.gov/gistemp/>), NOAA GlobTemp (<https://www.ncdc.noaa.gov/noaa->

255 [merged-land-ocean-global-surface-temperature-analysis-noaaglobaltemp-v5](#)), GPCP
 256 (<https://www.dwd.de/EN/ourservices/gpcc/gpcc.html>), HadUK-Grid
 257 (<http://catalogue.ceda.ac.uk/uuid/4dc8450d889a491ebb20e724debe2dfb>), MPI Large Ensemble
 258 (<https://www.mpimet.mpg.de/en/grand-ensemble/>).

259 **References**

- 260 Ashcroft, L., J. R. Coll, A. Gilabert, P. Domonkos, M. Brunet, E. Aguilar, M. Castella, J. Sigro,
 261 I. Harris, P. Uden and P. Jones, A rescued dataset of sub-daily meteorological
 262 observations for Europe and the southern Mediterranean region, 1877–2012, *Earth Syst.*
 263 *Sci. Data*, 10, 1613–1635doi: 10.5194/essd-10-1613-2018, 2018
- 264 Battisti, D. S., and R. L. Naylor, Historical warnings of future food insecurity with
 265 unprecedented seasonal heat, *Science*, 323(5911), 240–244, doi:10.
 266 1126/science.1164363, 2009.
- 267 Beaumont, L. J., A. Pitman, S. Perkins, N. E. Zimmermann, N. G. Yoccoz, and W. Thuiller,
 268 Impacts of climate change on the worlds most exceptional ecoregions, *Proceedings of the*
 269 *National Academy of Sciences*, 108 (6), 2306– 2311, doi:10.1073/pnas.1007217108,
 270 2011.
- 271 Boisier, J. P., R. Rondanelli, R. D. Garreaud, and F. Munoz, Anthropogenic and natural
 272 contributions to the southeast Pacific precipitation decline and recent megadrought in
 273 central Chile, *Geophysical Research Letters*, 43(1), 413–421, doi:10.1002/2015gl067265,
 274 2016.
- 275 Burt, S. and Burt, T., *Oxford Weather and Climate since 1767*, Oxford University Press, 2019
- 276 Callendar, G. S., The artificial production of carbon dioxide and its influence on temperature,
 277 *Quarterly Journal of the Royal Meteorological Society*, 64(275), 223–240,
 278 doi:10.1002/qj.49706427503, 1938.
- 279 Cowtan, K., and R. G. Way, Coverage bias in the HadCRUT4 temperature series and its impact
 280 on recent temperature trends, *Quarterly Journal of the Royal Meteorological Society*,
 281 140(683), 1935–1944, doi: 10.1002/qj.2297, 2014.
- 282 Delworth, T. L., and F. Zeng, Regional rainfall decline in Australia attributed to anthropogenic
 283 greenhouse gases and ozone levels, *Nature Geoscience*, 7(8), 583–587,
 284 doi:10.1038/ngeo2201, 2014.
- 285 Deutsch, C. A., J. J. Tewksbury, R. B. Huey, K. S. Sheldon, C. K. Ghalambor, D. C. Haak, and
 286 P. R. Martin, Impacts of climate warming on terrestrial ectotherms across latitude,
 287 *Proceedings of the National Academy of Sciences*, 105(18), 6668–6672,
 288 doi:10.1073/pnas.0709472105, 2008.
- 289 Diffenbaugh, N. S., and M. Scherer, Observational and model evidence of global emergence of
 290 permanent, unprecedented heat in the 20th and 21st centuries, *Climatic Change*, 107(3-4),
 291 615–624, doi:10.1007/ s10584-011-0112-y, 2011.
- 292 Diffenbaugh, N. S., M. Scherer and M. Ashfaq, Response of snow-dependent hydrologic
 293 extremes to continued global warming, *Nature Climate Change*, 3, 379, doi:
 294 10.1038/nclimate1732, 2013

- 295 Dima, M. and G. Lohmann, Evidence for Two Distinct Modes of Large-Scale Ocean Circulation
296 Changes over the Last Century, *Journal of Climate*, 23, 5, doi: 10.1175/2009JCLI2867.1,
297 2010
- 298 Fischer, E. M., J. Sedlacek, E. Hawkins, and R. Knutti, Models agree on forced response pattern
299 of precipitation and temperature extremes, *Geophysical Research Letters*, 41(23), 8554–
300 8562, doi:10.1002/2014gl062018, 2014.
- 301 Frame, D., M. Joshi, E. Hawkins, L. J. Harrington, and M. de Roiste, Population-based
302 emergence of unfamiliar climates, *Nature Climate Change*, 7(6), 407–411,
303 doi:10.1038/nclimate3297, 2017.
- 304 Giorgi, F., and X. Bi, Time of emergence (TOE) of GHG-forced pre- cipitation change hot-spots,
305 *Geophysical Research Letters*, 36(6), doi: 10.1029/2009gl037593, 2009.
- 306 Hansen, J., I. Fung, A. Lacis, D. Rind, S. Lebedeff, R. Ruedy, G. Russell, and P. Stone, Global
307 climate changes as forecast by Goddard institute for space studies three-dimensional
308 model, *Journal of Geophysical Research*, 93(D8), 9341, doi:10.1029/jd093id08p09341,
309 1988.
- 310 Harrington, L., D. Frame, E. Hawkins and M. Joshi, Seasonal cycles enhance disparities between
311 low- and high-income countries in exposure to monthly temperature emergence with
312 future warming, *Environ. Res. Lett.*, 12, 114039, doi: 10.1088/1748-9326/aa95ae, 2017
- 313 Haustein, K., M. R. Allen, P. M. Forster, F. E. L. Otto, D. M. Mitchell, H. D. Matthews, and D.
314 J. Frame, A real-time global warming index, *Scientific Reports*, 7(1),
315 doi:10.1038/s41598-017-14828-5, 2017.
- 316 Hawkins, E., and R. Sutton, Time of emergence of climate signals, *Geophysical Research*
317 *Letters*, 39 (1), doi:10.1029/2011gl050087, 2012.
- 318 Hawkins, E., S. Burt, P. Brohan, M. Lockwood, H. Richardson, M. Roy, and S. Thomas, Hourly
319 weather observations from the Scottish highlands (1883–1904) rescued by volunteer
320 citizen scientists, *Geoscience Data Journal*, doi:10.1002/gdj3.79, 2019.
- 321 Hollis, D., M. McCarthy, M. Kendon, T. Legg, and I. Simpson, HadUK-grid—a new UK dataset
322 of gridded climate observations, *Geoscience Data Journal*, doi:10.1002/gdj3.78, 2019.
- 323 IPCC, Summary for Policymakers. In: *Global Warming of 1.5°C. An IPCC Special Report on*
324 *the impacts of global warming of 1.5°C above pre-industrial levels and related global*
325 *greenhouse gas emission pathways, in the context of strengthening the global response to*
326 *the threat of climate change, sustainable development, and efforts to eradicate poverty*
327 *[Masson-Delmotte, V., P. Zhai, H.-O. Pörtner, D. Roberts, J. Skea, P.R. Shukla, A.*
328 *Pirani, W. Moufouma-Okia, C. Péan, R. Pidcock, S. Connors, J.B.R. Matthews, Y. Chen,*
329 *X. Zhou, M.I. Gomis, E. Lonnoy, T. Maycock, M. Tignor, and T. Waterfield (eds.)].*
330 *World Meteorological Organization, Geneva, Switzerland, 32 pp., 2018*
- 331 Kennedy, J. J., N. A. Rayner, R. O. Smith, D. E. Parker, and M. Saunby, Reassessing biases and
332 other uncertainties in sea surface temperature observations measured in situ since 1850:
333 1. measurement and sampling uncertainties, *Journal of Geophysical Research*, 116(D14),
334 doi:10.1029/ 2010jd015218, 2011.

- 335 Kincer, J. B., Is our climate changing? A study of long-time temperature trends, *Monthly*
336 *Weather Review*, 61 (9), 251–259, doi:10.1175/1520-0493(1933)61(251:ioccas)2.0.co;2,
337 1933.
- 338 King, A. D., and L. J. Harrington, The inequality of climate change from 1.5 to 2c of global
339 warming, *Geophysical Research Letters*, 45 (10), 5030–5033,
340 doi:10.1029/2018gl078430, 2018.
- 341 King, A. D., M. G. Donat, E. M. Fischer, E. Hawkins, L. V. Alexander, D. J. Karoly, A. J.
342 Dittus, S. C. Lewis, and S. E. Perkins, The timing of anthropogenic emergence in
343 simulated climate extremes, *Environmental Research Letters*, 10(9), 094,015,
344 doi:10.1088/1748-9326/10/9/094015, 2015.
- 345 Lehner, F., C. Deser, and L. Terray, Toward a new estimate of “time of emergence” of
346 anthropogenic warming: Insights from dynamical adjustment and a large initial-condition
347 model ensemble, *Journal of Climate*, 30(19), 7739–7756, doi:10.1175/jcli-d-16-0792.1,
348 2017.
- 349 Lenssen, N. J. L., G. A. Schmidt, J. E. Hansen, M. J. Menne, A. Persin, R. Ruedy, and D. Zyss,
350 Improvements in the GISTEMP uncertainty model, *Journal of Geophysical Research:*
351 *Atmospheres*, 124(12), 6307–6326, doi: 10.1029/2018jd029522, 2019.
- 352 Madden, R. A., and V. Ramanathan, Detecting climate change due to in- creasing carbon
353 dioxide, *Science*, 209 (4458), 763–768, doi:10.1126/science. 209.4458.763, 1980.
- 354 Maher, N., et al., The Max Planck Institute grand ensemble: Enabling the exploration of climate
355 system variability, *Journal of Advances in Modeling Earth Systems*, 11(7), 2050–2069,
356 doi:10.1029/2019ms001639, 2019.
- 357 Mahlstein, I., R. Knutti, S. Solomon, and R. W. Portmann, Early onset of significant local
358 warming in low latitude countries, *Environmental Research Letters*, 6(3), 034,009,
359 doi:10.1088/1748-9326/6/3/034009, 2011.
- 360 Mahlstein, I., G. Hegerl, and S. Solomon, Emerging local warming signals in observational data,
361 *Geophysical Research Letters*, 39 (21), doi: 10.1029/2012gl053952, 2012.
- 362 Mahlstein, I., J. S. Daniel, and S. Solomon, Pace of shifts in climate regions increases with
363 global temperature, *Nature Climate Change*, 3, 739, doi: 10.1038/nclimate1876, 2013
- 364 Min, S.-K., X. Zhang, F. W. Zwiers, and G. C. Hegerl, Human contribution to more-intense
365 precipitation extremes, *Nature*, 470(7334), 378–381, doi: 10.1038/nature09763, 2011.
- 366 Monllor-Hurtado, A., M. G. Pennino, and J. L. Sanchez-Lizaso, Shift in tuna catches due to
367 ocean warming, *PLOS ONE*, 12(6), e0178,196, doi: 10.1371/journal.pone.0178196,
368 2017.
- 369 Morice, C. P., J. J. Kennedy, N. A. Rayner, and P. D. Jones, Quantifying uncertainties in global
370 and regional temperature change using an ensemble of observational estimates: The
371 HadCRUT4 data set, *Journal of Geophysical Research: Atmospheres*, 117(D8), n/a–n/a,
372 doi:10.1029/2011jd017187, 2012.
- 373 Pall, P., M. R. Allen & D. A. Stone, Testing the Clausius–Clapeyron constraint on changes in
374 extreme precipitation under CO₂ warming, *Climate Dynamics*, 28, 351, doi:
375 10.1007/s00382-006-0180-2, 2007

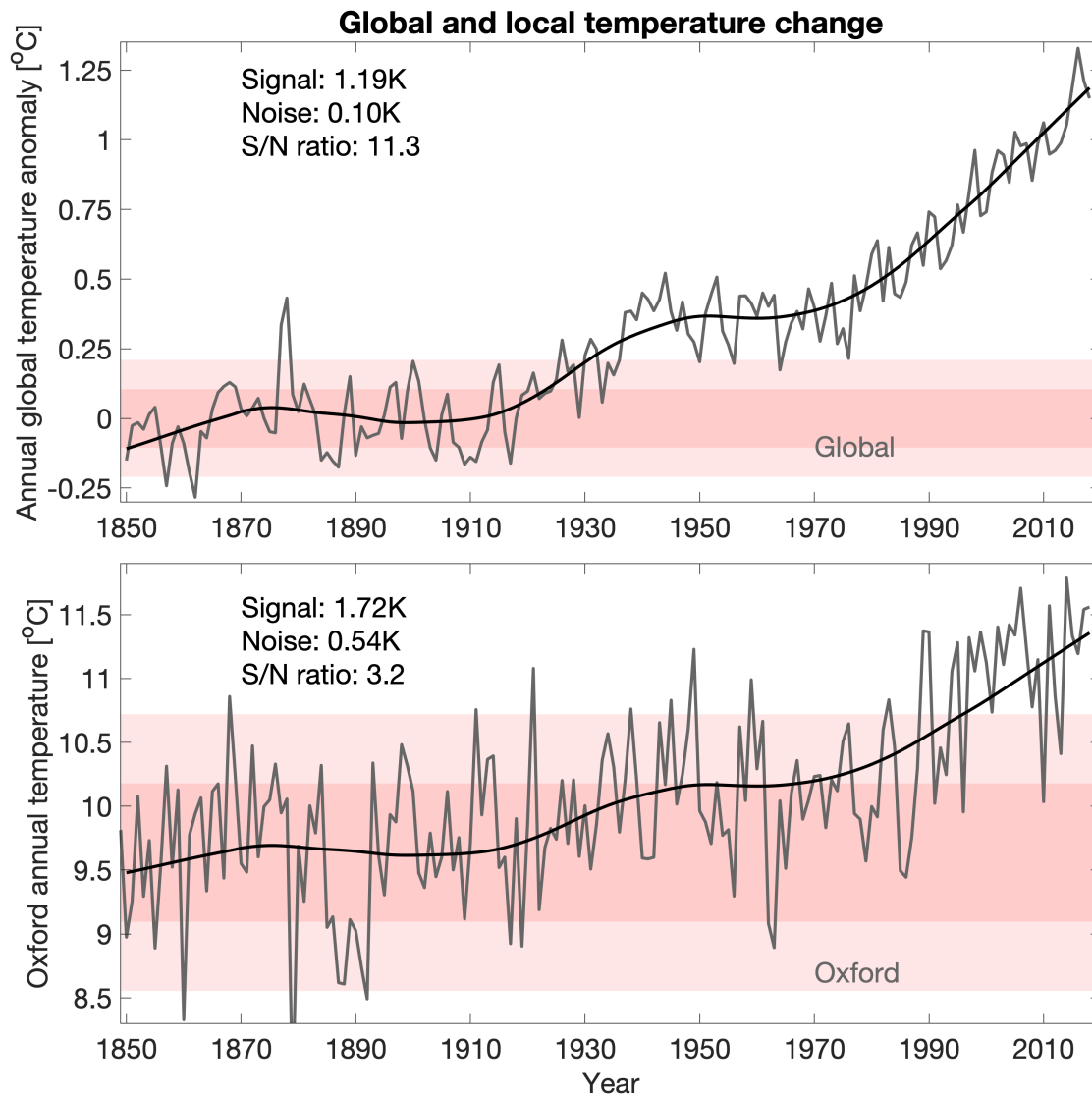
- 376 Rohde, R., R. A. Muller, R. Jacobsen, E. Muller, S. Perlmutter, A. Rosenfeld, J. Wurtele, D.
377 Groom and C. Wickham, A New Estimate of the Average Earth Surface Land
378 Temperature Spanning 1753 to 2011, *Geoinfor Geostat*, 1, 1, doi:10.4172/2327-
379 4581.1000101, 2013
- 380 Rojas, M., F. Lambert, J. Ramirez-Villegas, and A. J. Challinor, Emergence of robust
381 precipitation changes across crop production areas in the 21st century, *Proceedings of the*
382 *National Academy of Sciences*, 116 (14), 6673–6678, doi:10.1073/pnas.1811463116,
383 2019.
- 384 Schneider, U., P. Finger, A. Meyer-Christoffer, E. Rustemeier, M. Ziese, and A. Becker,
385 Evaluating the hydrological cycle over land using the newly- corrected precipitation
386 climatology from the global precipitation climatology centre (GPCC), *Atmosphere*,
387 8(12), 52, doi:10.3390/atmos8030052, 2017.
- 388 Sutton, R., E. Suckling, and E. Hawkins, What does global mean tempera- ture tell us about local
389 climate?, *Philosophical Transactions of the Royal Society A: Mathematical, Physical and*
390 *Engineering Sciences*, 373(2054), 20140,426, doi:10.1098/rsta.2014.0426, 2015.
- 391 Thirumalai, K., P. N. DiNezio, Y. Okumura, and C. Deser, Extreme temperatures in southeast
392 Asia caused by El Nino and worsened by global warming, *Nature Communications*, 8(1),
393 doi:10.1038/ncomms15531, 2017.
- 394 Wigley, T. M. L. and P. D. Jones, Detecting CO₂-induced climatic change, *Nature*, 292, 205,
395 1981
- 396 Zappa, G. and T.G. Shepherd, Storylines of Atmospheric Circulation Change for European
397 Regional Climate Impact Assessment. *J. Climate*, 30, 6561–6577, doi: 10.1175/JCLI-D-
398 16-0807.1, 2017
- 399 Zhang, H.-M., et al., Updated temperature data give a sharper view of climate trends, *Eos*, 100,
400 doi:10.1029/2019eo128229, 2019.
- 401 Zhang, X., F. W. Zwiers, G. C. Hegerl, F. H. Lambert, N. P. Gillett, S. Solomon, P. A. Stott, and
402 T. Nozawa, Detection of human influence on twentieth-century precipitation trends,
403 *Nature*, 448(7152), 461–465, doi: 10.1038/nature06025, 2007.

404

405

406

407

408
409

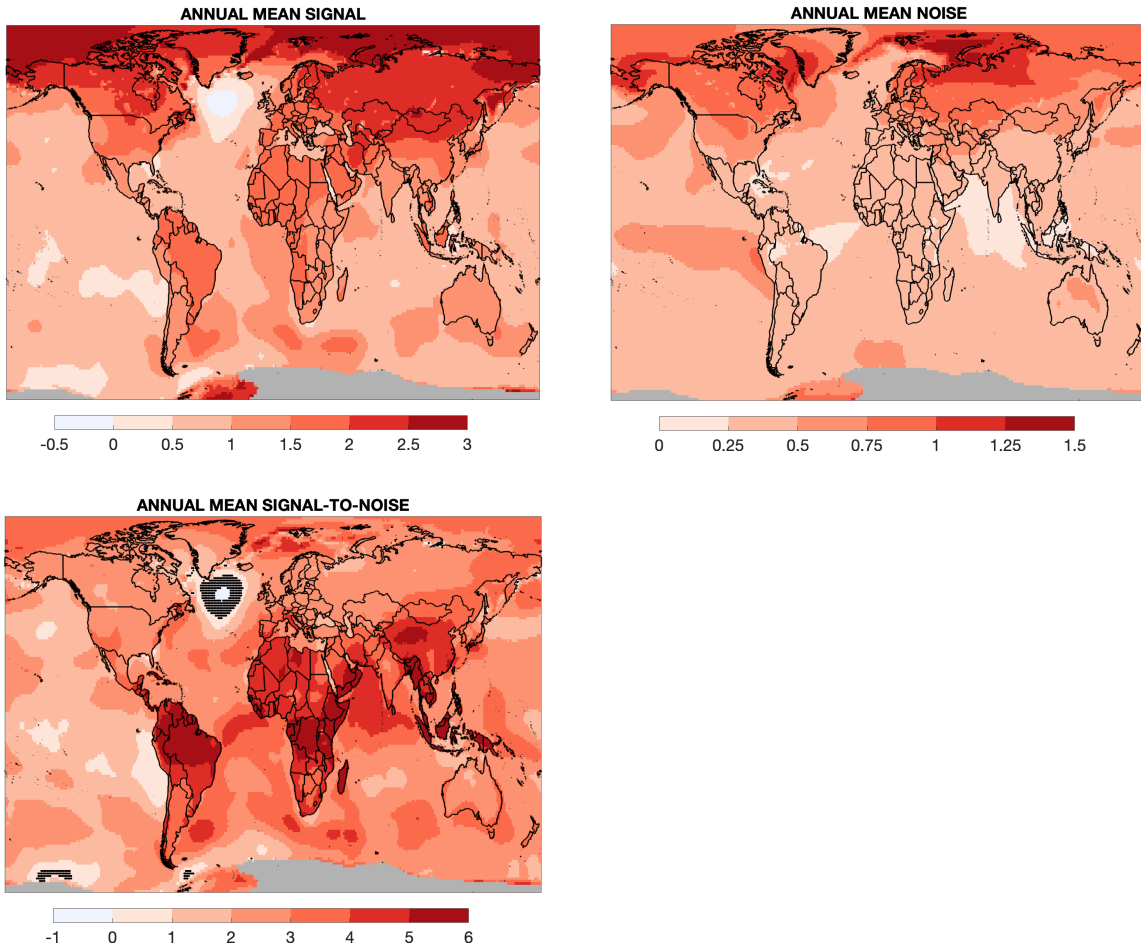
410

411 **Figure 1:** Emergence of global and local temperature change from 1850-2018. (top) GMST
 412 (grey), smoothed with a 41-year lowess filter (black). (bottom) Oxford annual temperature (grey)
 413 and scaled smoothed GMST (black). The correlation between Oxford temperatures and
 414 smoothed GMST is 0.67, and if the Oxford data is also smoothed with a 41-year lowess filter the
 415 correlation increases to 0.98. The shaded bands indicate 1 and 2 standard deviations of the noise.
 416 Fig. S2 shows other regional examples.

417

418

419

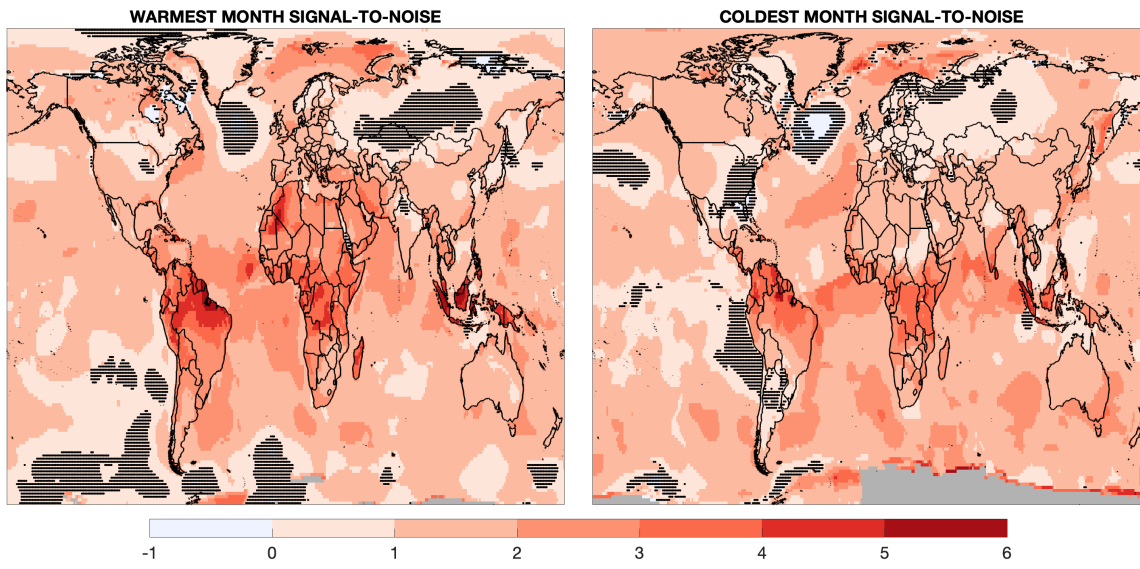


420

421

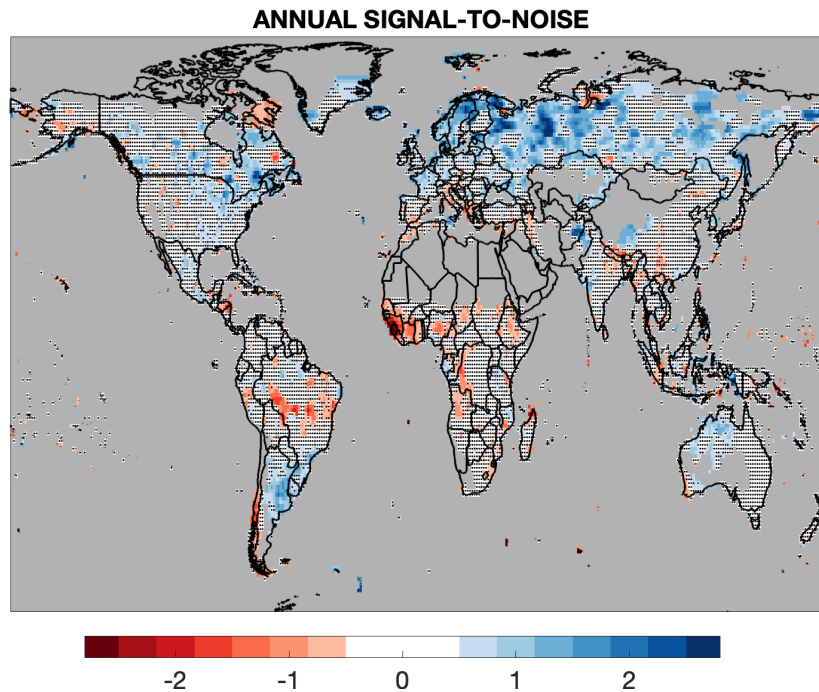
422 **Figure 2:** Signal, noise (both in K) and S/N for observed annual mean temperature change in the
 423 Berkeley Earth dataset. Many tropical regions show the smallest signal, but also the smallest
 424 noise and largest S/N. Grey regions denote lack of sufficient data. The S/N values in stippled
 425 areas are not significantly different from zero.

426



427

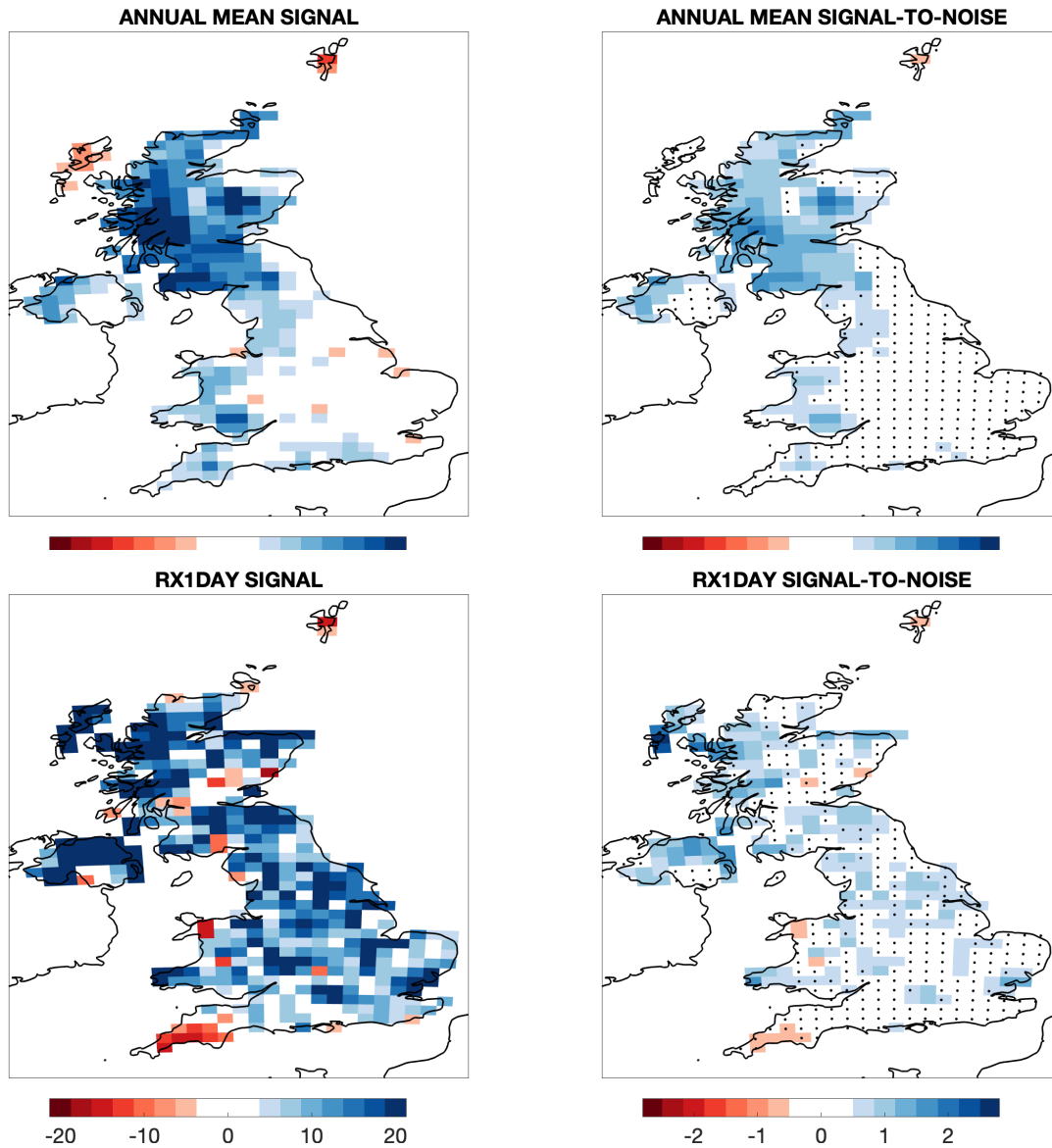
428 **Figure 3:** Signal-to-noise ratio for monthly average temperatures, for the climatologically
 429 warmest (left) and coldest (right) months at each grid point. Grey regions denote lack of
 430 sufficient data. The S/N values in stippled areas are not significantly different from zero.



431

432 **Figure 4:** Signal-to-noise ratio for annual mean precipitation over land using the GPCP dataset.
 433 Blue colours denote regions becoming wetter, and red colours denote regions that are becoming
 434 drier. Grey regions are either unobserved (oceans) or deserts (<250mm/year). Stippling indicates
 435 where the regression parameter is not statistically significant from zero.

436



437

438

439 **Figure 5:** Signal (left) and signal-to-noise ratio (right) for annual mean precipitation over the UK (top row, 1862-
 440 2017) and extreme daily rainfall (RX1day, bottom row, 1891-2017) using the HadUK-Grid dataset. The signal is
 441 presented in units of % per K of GMST change. Blue colours denote regions becoming wetter, and red colours
 442 denote regions that are becoming drier. Stippling in the S/N panels indicates where the regression parameter is not
 443 statistically significant from zero.

444